



# EEG based emotion recognition using minimum spanning tree

Sajjad Farashi<sup>1,2</sup> · Reza Khosrowabadi<sup>3</sup>

Received: 12 November 2019 / Accepted: 29 June 2020

© Australasian College of Physical Scientists and Engineers in Medicine 2020

## Abstract

Emotion is a fundamental factor that influences human cognition, motivation, decision making and social interactions. This psychological state arises spontaneously and goes with physiological changes that can be recognized by computational methods. In this study, changes in minimum spanning tree (MST) structure of brain functional connectome were used for emotion classification based on EEG data and the obtained results were employed for interpretation about the most informative frequency content of emotional states. For estimation of interaction between different brain regions, several connectivity metrics were applied and interactions were calculated in different frequency bands. Subsequently, the MST graph was extracted from the functional connectivity matrix and its features were used for emotion recognition. The results showed that the accuracy of the proposed method for separating emotions with different arousal levels was 88.28%, while for different valence levels it was 81.25%. Interestingly, the system performance for binary classification of emotions based on quadrants of arousal-valence space was also higher than 80%. The MST approach allowed us to study the change of brain complexity and dynamics in various emotional states. This capability provided us enough knowledge to claim lower-alpha and gamma bands contain the main information for discrimination of emotional states.

**Keywords** Emotion recognition · Minimum spanning tree · Graph theory · Electroencephalography · Arousal-valence space · Pattern recognition

## Introduction

Automatic emotion recognition by means of computerized algorithms has gained special attention during the last decade. Emotion recognition is necessary for developing brain-machine or brain-computer interfaces for disabled people who have no ability to express their emotions using voice or facial expression [1]. In addition, in neuromarketing understanding customer interest in specific products using emotion recognition techniques is an attractive issue [2, 3]. Moreover, emotion recognition has been used in many medical and

social researches such as studies on depression [4], Parkinson's disease [5] and autism spectrum disorder [6]. Overall, investigation of brain mechanisms involved in the process of emotional stimuli and using automatic techniques to discriminate emotional states has been the subject of several studies [7, 8]. So far, various measurement techniques have been applied for this purpose. For instance, emotion recognition from facial expression has been used in several studies [9, 10]. Some other researchers have used peripheral physiological data such as blood pressure [11], hemodynamic data acquired by fNIRS [12], electrocardiography signal (ECG) [13], speech [14], skin conductance and electromyography [15] and the combination of these signals [16]. Among these techniques, electroencephalography (EEG) which measures brain electrical activities has been one of the most interesting tools for emotion recognition [17]. In several ways, the information regarding emotional states has been extracted from EEG signals such as event-related potential [18, 19], laterality of activities in the prefrontal cortex [20], Gaussian mixture models of power spectrum [21], mel-frequency cepstrum coefficients [22], bispectrum [23], short term Fourier transform [24], artificial neural network [25], energy and

**Electronic supplementary material** The online version of this article (<https://doi.org/10.1007/s13246-020-00895-y>) contains supplementary material, which is available to authorized users.

✉ Sajjad Farashi  
[sajjad\\_farashi@yahoo.com](mailto:sajjad_farashi@yahoo.com)

<sup>1</sup> Hamadan University of Medical Sciences, Hamadan, Iran

<sup>2</sup> Autism Spectrum Disorder Research Center, Hamadan University of Medical Sciences, Hamadan, Iran

<sup>3</sup> Institute for Cognitive and Brain Sciences, Shahid Beheshti University GC, Tehran, Iran

entropy of wavelet coefficients [26] which both are useful measures for neural data processing [27, 28], sample entropy of intrinsic mode functions derived from empirical mode decomposition method [29], fractal dimension [30] and zero-order crossing of EEG signal [31]. Changes in the pattern of functional connectivity between different regions of the brain have also been used for emotion recognition and various approaches including correlation [32], coherence [33], mutual information [34], phase synchronization indices [35] and weighted phase lag index [36] have been investigated for this purpose. The extracted features are usually fed to the famous classifiers such as support vector machine (SVM) and fuzzy C-means [3, 37, 38].

In a connectivity approach, brain functions are considered to arise from synchronized activity (edges) of several information processing nodes (vertices). In this regard, a graph theoretical approach can be used for functional analysis. In a graph, the backbone structure behind brain-specific behavior such as the perception of emotional stimuli can be evaluated by the minimum spanning tree (MST). It has been used for analyzing the brain network of children with math difficulties [39], dyslexic readers [40], amyotrophic lateral sclerosis disease [41], understanding sub-networks for the distinction of subject traits [42], discrimination of motor imagery hand movement [43], testing cognitive impairment in dementia [44] and investigation of changes in the brain functional networks after surgery [45].

In this paper, the MST was constructed from EEG data recorded in several emotional states. Besides the structure of the brain functional connectome during the process of emotional stimuli, the role of different frequency bands in the process of emotions was also investigated. In this approach, it was assumed that brain waves had their own specific roles for information processing in different tasks [46]. This idea has been the subject of several studies, for instance, certain types of attention are associated with alpha-band activities [46], working memory functions are mainly produced in theta-band [47] and during learning and memory, the coupling between high-frequency oscillations, i.e. theta and gamma waves, is also well known [48]. In this regard, Muller et al. have also shown that differences in emotional states are more prominent in the gamma-band range [49]. It has been confirmed by Luo et al. that have reported an increase of event-related synchronization in the gamma band spectrum in response to emotional excitation compared with neutral state [50]. Therefore, in this study, we hypothesized that the backbone of the brain functional network was significantly changed while the person processes emotional stimuli as compared to the neutral state. In addition, it was hypothesized that this phenomenon occurred in a frequency-specific manner. Using a two-dimensional arousal-valence space model [51] (see Fig. 1), our main purpose was to find out the most informative frequency band for valence and

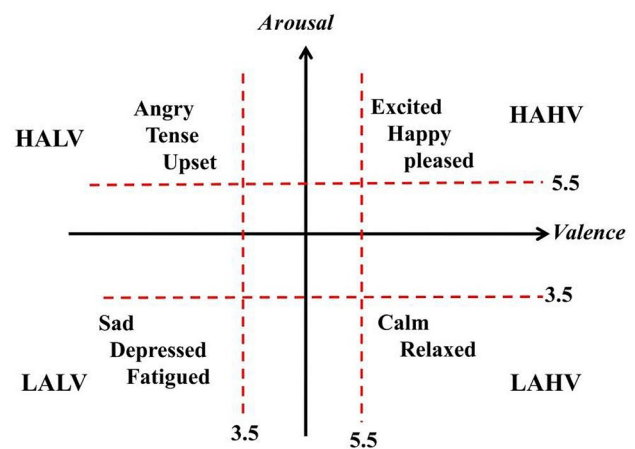


**Fig. 1** Two-dimensional (arousal-valence) emotion space. Four quadrants have been defined according to the combined level of arousal or valence. HALV refers to high arousal-low valence, HAHV refers to high arousal-high valence, LALV refers to low arousal-low valence and LAHV refers to low arousal-high valence level

arousal levels using graph theoretical approach. The results may help researchers to propose a more reliable therapeutic method for emotion-related diseases.

## Material and methods

### Dataset description

In this paper, a dataset for emotion analysis using physiological signals (DEAP) [52] was used which was publicly available. The dataset consisted of EEG and other peripheral physiological signals of 32 subjects (mean = 29.6 years old, 16 females) that had been recorded while the subjects were exposed to 40 one minute video clips with emotional content. In the present work, only the EEG data were used for testing and evaluation of the proposed method for emotional state analysis. The EEG data had been recorded using a 10–20 system with a sampling rate of 512 Hz that were down-sampled to 128 Hz during the analysis. In DEAP dataset, a subject self-rating mechanism was used to label each trial according to the arousal, valence, like/dislike, dominance and familiarity of the video clips. In order to reduce the complexity of the emotion classification task, only two main dimensions of arousal and valence had been considered in this study.

The EEG data of each channel was filtered using a band-pass filter in 4–45 Hz. In addition, to investigate the effects of each frequency band separately, the EEG data were also separated into different frequency bands including theta: 4–7.5 Hz, alpha1: 8–10 Hz, alpha2: 10.5–13 Hz, beta: 13–30 Hz and gamma: 31–45 Hz. The alpha frequency band was divided into two ranges because it was believed that the

lower and upper ranges reflected different aspects of brain functions [53, 54]. In addition, since two different electrode configurations were used in the collection of DEAP dataset (Geneva and Twente), therefore, EEG data matrices were rearranged to compensate for such differences.

## Proposed method

The main purpose of this paper was to distinguish between different emotions using the extracted features of MST graph. For each subject, the selected segments of EEG recordings were used to create brain connectivity matrix and its associated MST graph. The block diagram of the proposed method was presented in Fig. 2. For analyzing brain functions using EEG signals, it was necessary to select appropriate segments of data which were correlated with the intended emotional state. In a more clear explanation, the emotional effect of watching a video clip might be limited to a small time span and not whole watching period. Therefore, the limited sample points of recorded EEG time-series should affect by changing emotional states. In this paper, the appropriate segments had been selected based on entropy measure. As it was shown in the supplementary material (Table S1), the entropy content of EEG signal was different between distinct emotional states. In this regard, two segments of EEG recordings, where the entropy content was

maximized, had been selected for further analysis. Besides the segmentation strategy, the length of the selected segment was of crucial importance. In case of very large segments, brain specific function and EEG signal may be unrelated [55], while in very small segments the information contained in the segment might not express the emotional state completely. For considering this issue, three different window sizes (2 s, 5 s and 10 s) were chosen. Interestingly, Candra et al. had also shown that an optimal window size of 3–10 and 3–12 s preserved the main information of arousal and valence levels, respectively [56]. Subsequently, after segmentation, the drift of each channel was removed by subtracting the average of the first 3 s segment (in case of 2 s segment drift was calculated based on the first 1 s points of the segment) from values of the channel. The drift value could affect the connectivity values and made the interpretation unreliable. Moreover, in order to make the interpretation more reliable, the connectivity matrices of several similar excitations were averaged for creating MST graph. Significant extracted features from MST graph were selected based on two-sample Kolmogorov–Smirnov test and were fed to the classifiers. The classification was performed using support vector machine (SVM) and quadratic discriminant analysis (QDA) methods.

## Brain connectivity metrics

The precise coordination of different brain regions is necessary for the correct functioning of the brain. Following the activation of neurons at specific brain areas, the electrical activity propagates toward the scalp. EEG is a non-invasive and inexpensive method for capturing such propagated electrical activities at the scalp and evaluates the synchronization of brain regions by comparing the electrical activities in a pair-wise manner. There are several methods for measuring the synchronization between different brain regions. The correlation coefficient shows the similarity between two time series in the time domain, while such coordination in the frequency domain is obtained using coherence [57]. The correlation metric calculates the linear relationship between two time-series while the interaction between brain regions may follow a nonlinear process. Unlike the correlation measure, mutual information considers the linear and nonlinear interactions between two time-series [58]. However, the correlation, coherence and mutual information metrics are all sensitive to volume conduction properties of the brain, where the activity of a unique source may be observed by several electrodes on the scalp. For reducing such sensitivity, several methods such as partial correlation [59], imaginary part of coherence [60], phase lag index [61], weighted phase lag index [62] and phase slope index [63] have been proposed so far. Therefore, correlation (Corr), partial correlation (Pcorr),

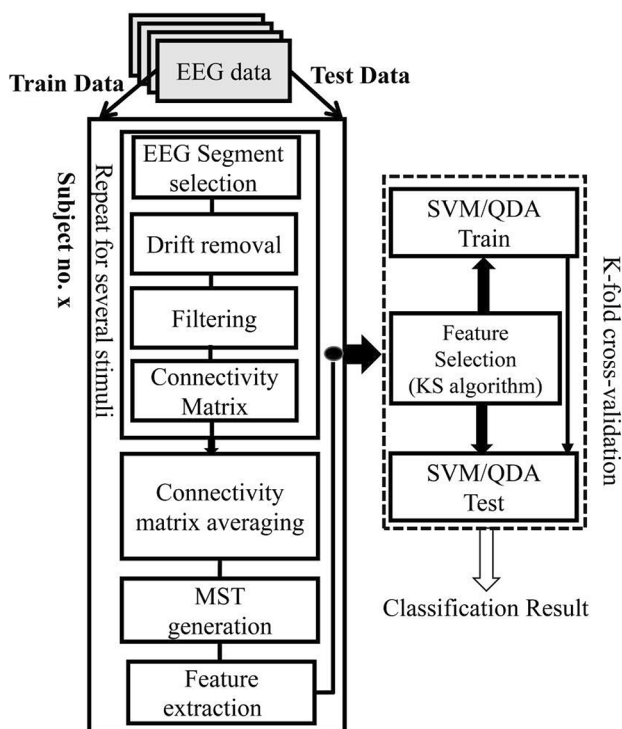


Fig. 2 Block diagram of the proposed method

mutual information (MI), phase lag index (PLI), weighted phase lag index (WPLI) and phase slope index (PSI) were implemented in this paper to evaluate the synchronization of different brain regions.

For calculating each element of the connectivity matrix, the pair-wise comparison between the time-series of EEG channels was calculated considering the above-mentioned connectivity measures. In this regard, the connectivity matrix was a symmetric matrix.

### MST measures

MST is a graph that vertices are connected together using a subset of edges, without the construction of any cycles [64]. In MST the total weight of edges is the minimum value between all possible configurations. From such a structure, the measures described in Table 1 are computed.

Betweenness centrality (BC) [65] is a quantitative measure that determines to what extent a node contributes to connect other nodes to each other. The higher centrality of a node means that the node has more control over the network and higher capability to affect the information flow in the network. In star-like trees, the central node has the maximum value of BC while the diameter of the network is minimal. In such a structure, the central node has maximum overload and its destruction causes the structure to collapse.

Hierarchy (H) is defined according to the following formula [66].

$$H = \frac{L}{2M(BC_{max})} \quad (1)$$

In which,  $L$  is leaf number and  $M$  is the number of edges in the tree. After the calculation of MST metrics, the most significant features were determined (see the next section).

### Statistical analysis

The dataset that we used in this study (DEAP dataset) contained the EEG data for 32 participants, therefore, 32 was the highest possible sample size for this study. In general, determining the suitable sample size for reliable statistical analysis is highly dependent on several parameters such as the power of the statistical analysis, the variance of samples in each group, type of test, effect size and confidence interval. For example, a sample size calculation for a model experimental design considering ANOVA, proposed the minimum of 28 subjects, in order to have a minimum power of 0.8, the minimum effect size of 0.25 and a significance level of 0.05, while sphericity assumption was satisfied [67]. For larger effect size larger sample size is needed.

In this study, features in which their distribution among all subjects showed a non-unimodal distribution were selected to be fed to our binary classifiers. To select such features, one-sample Kolmogorov–Smirnov test was used according to Eq. 2.

$$D = \max|F(x) - G(x)| \quad (2)$$

where  $F(x)$  denoted the cumulative distribution function (CDF) of each feature vector and  $G(x)$  presented the CDF of a Gaussian distribution (unimodal) with the same mean and standard deviation of the feature vector. A higher distance from the unimodal distribution implied that the selected feature distinguished two classes in a better manner. In order to highlight statistically significant differences, p-value statistic calculated using Wilcoxon sign-ranked test or two-sample t-test was considered.

### Results

In this section, the results for the performance of the proposed method for emotion recognition were reported. For discrimination between emotional states, SVM and QDA classifiers were used. The obtained results (not shown here) showed that both classifiers obtained nearly similar outcome,

**Table 1** MST graph measures

Measure	Description
Degree (k)	Number of neighbors of each node
Diameter (d)	Longest path between nodes in MST structure
Eccentricity (E)	Longest path between each node and any other nodes. This measure is defined for each node
Leaf number (L)	Number of nodes with a degree of one
Radius (R)	Minimum value of eccentricity of vertices
Betweenness centrality (BC)	Amount of centrality of a node in the graph
Hierarchy (H)	Determines a trade-off between diameter and Betweenness Centrality

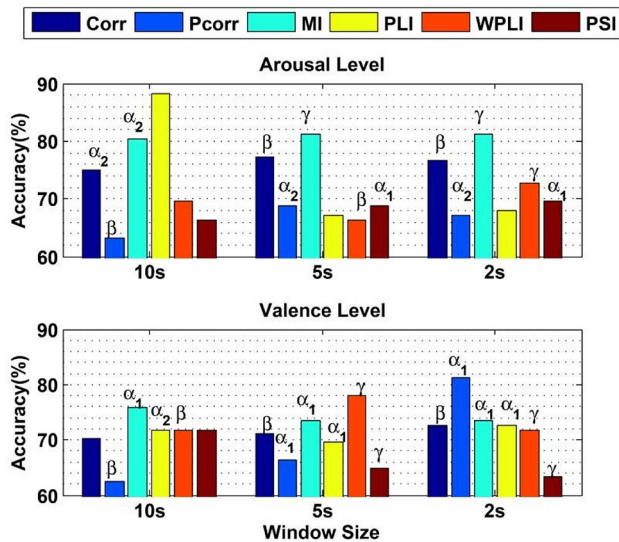


**Fig. 3** Classification accuracy based on the arousal (upper panel) and valence (lower panel) levels. The frequency band, where maximum accuracy was obtained, was indicated above each bar, except where the maximum accuracy was obtained using the whole frequency spectrum of EEG time-series

however, here the best result was reported. The discrimination accuracy of the proposed method was evaluated in various frequency bands using different connectivity metrics and the results were depicted in Fig. 3.

The accuracy of binary classification for distinguishing different emotional states, which categorized into four quadrants of arousal-valence space (see Fig. 1), was reported in Table 2.

Furthermore, the accuracy of the proposed method was compared with some other state-of-the-art methods in Table 3.

In searching for the most important frequency bands for brain emotion processing, the obtained results by classification by the proposed method were used and some proven facts from the literature were incorporated. In fact, the purpose of these further analyses was to choose the frequency bands where the obtained results by MST followed the reported experimental outcomes. Figures 4, 5 and 6 contained the results of these analyses.

In Fig. 4, the average betweenness centrality of MST graphs among all subjects in DEAP dataset was calculated (each graph was constructed by averaged connectivity matrices obtained by trials tagged as LALV according to

**Table 2** Classification accuracy (%) for binary classification according to arousal-valence space

Classification/method	Corr	Pcorr	MI	PLI	WPLI	PSI
LAHV/HAHV	$\beta$ 79.99( $\pm 1.31$ )	$\gamma$ 68.75( $\pm 3.49$ )	$\beta$ 74.06( $\pm 1.78$ )	<b>*</b> <b>80.93(<math>\pm 1.31</math>)</b>	$\alpha_1$ 72.49( $\pm 1.40$ )	$\alpha_1$ 68.43( $\pm 1.31$ )
HAHV/HALV	$\alpha_1$ 68.71( $\pm 4.77$ )	$\gamma$ 67.78( $\pm 2.32$ )	$\gamma$ 67.49( $\pm 1.31$ )	$\alpha_1$ 72.49( $\pm 1.40$ )	$\beta$ 75.94( $\pm 1.78$ )	<b>*</b> <b>83.12(<math>\pm 1.71</math>)</b>
HAHV/LALV	$\gamma$ 83.12( $\pm 0.70$ )	$\beta$ 74.37( $\pm 2.84$ )	<b><math>\gamma</math></b> <b>90.00(<math>\pm 0.85</math>)</b>	<b>*</b> 81.25( $\pm 1.56$ )	<b>*</b> 78.44( $\pm 2.57$ )	$\beta$ 64.06( $\pm 1.10$ )
LAHV/HALV	$\beta$ 72.50( $\pm 1.40$ )	$\theta$ 73.12( $\pm 2.32$ )	<b>*</b> 80.21( $\pm 1.60$ )	<b><math>\alpha_2</math></b> <b>89.06(<math>\pm 1.91</math>)</b>	$\beta$ 73.75( $\pm 1.31$ )	<b>*</b> 84.69( $\pm 1.31$ )
HALV/LALV	<b>*</b> 84.37( $\pm 0.00$ )	$\theta$ 69.06( $\pm 1.30$ )	<b><math>\gamma</math></b> <b>90.31(<math>\pm 0.70</math>)</b>	<b>*</b> 87.17( $\pm 1.31$ )	<b>*</b> 88.12( $\pm 2.84$ )	<b>*</b> 75.62( $\pm 1.40$ )
LAHV/LALV	$\alpha_1$ 84.68( $\pm 0.70$ )	$\alpha_2$ 68.12( $\pm 2.61$ )	<b><math>\alpha_1</math></b> <b>88.75(<math>\pm 1.30</math>)</b>	$\alpha_2$ 81.56( $\pm 0.70$ )	<b>*</b> 87.19( $\pm 1.30$ )	$\beta$ 76.59( $\pm 1.1$ )

Asterisks indicated that the result was obtained using the whole frequency spectrum of EEG time-series. Values were mean ( $\pm$  SD) which obtained using ten-fold cross-validation by SVM or QDA classifiers. The maximum value between different frequency bands was highlighted

**Table 3** Comparison between different classification algorithms for emotion recognition using DEAP dataset

Method	Feature	Classifier	Accuracy (%)	Ref.
Power spectral	Power of different EEG waves	Bayes classifier	Arousal: 62 Valence: 57.6	[52]
Wavelet	Entropy and energy of wavelet coefficients	SVM and KNN	Arousal: 86.75 Valence: 84.05	[26]
Entropy	Sample entropy	SVM	Arousal: 79.11 Valence: 80.43	[68]
Minimum spanning tree	Graph characteristic features	QDA and SVM	Arousal: 88.28 Valence: 81.25	This work



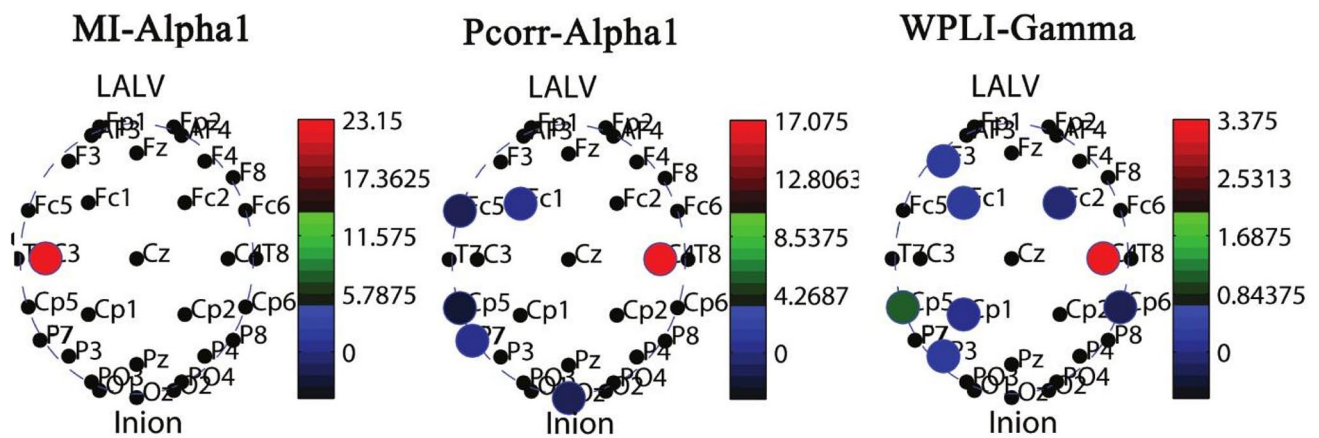


**Fig. 4** Pattern of betweenness centrality for emotions with low valence level (negative emotions), where maximum accuracy was achieved for separating low and high valence levels (see Fig. 3, lower

panel). Only the nodes in which their betweenness centrality was higher than average betweenness centrality of all nodes were shown. The allocated color to each node indicated the hubness of that node

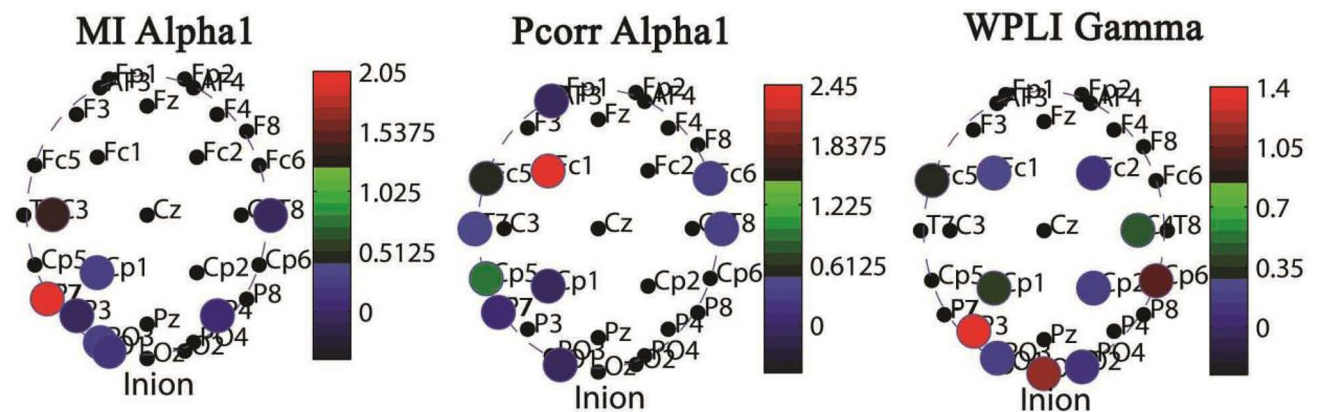


**Fig. 5** Pattern of betweenness centrality for emotions with high valence level (positive emotions). According to the result in Fig. 3 (lower panel), window size, frequency band and connectivity metric

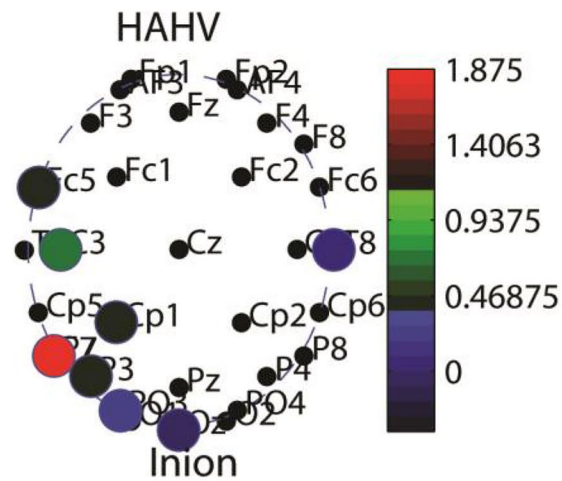
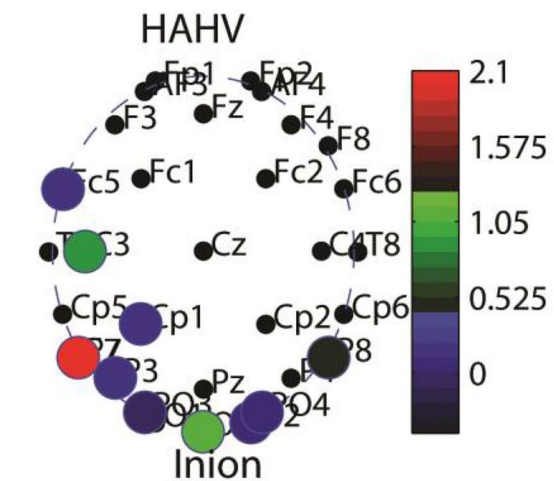
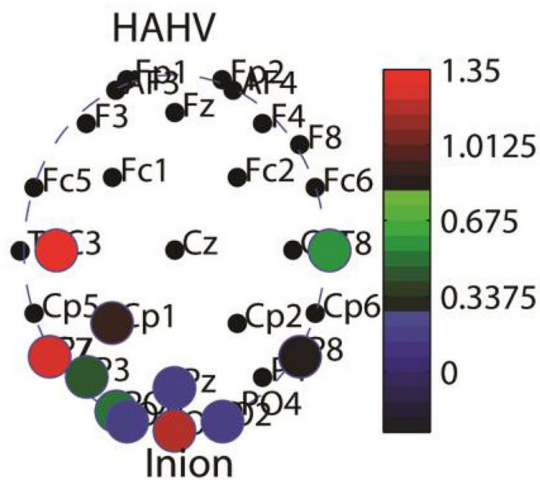
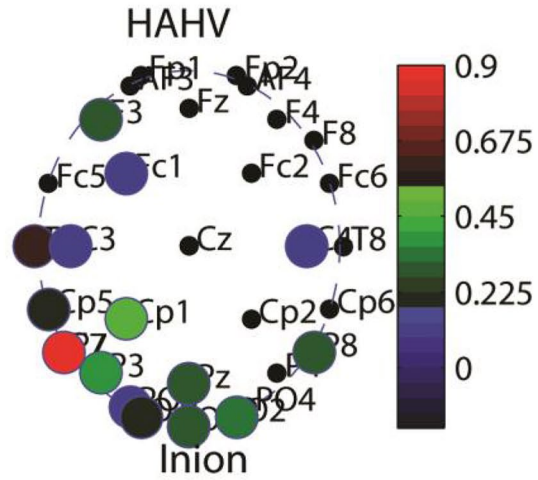
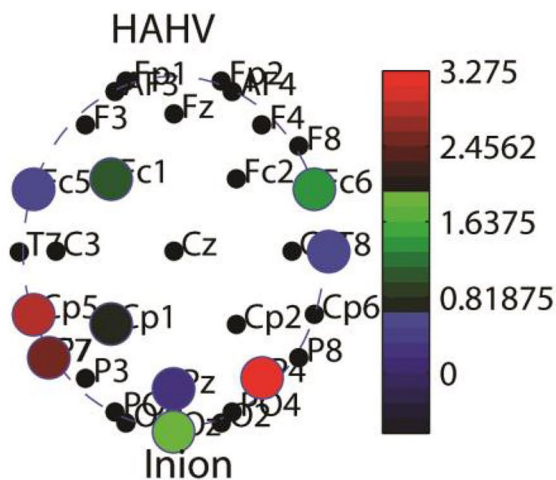
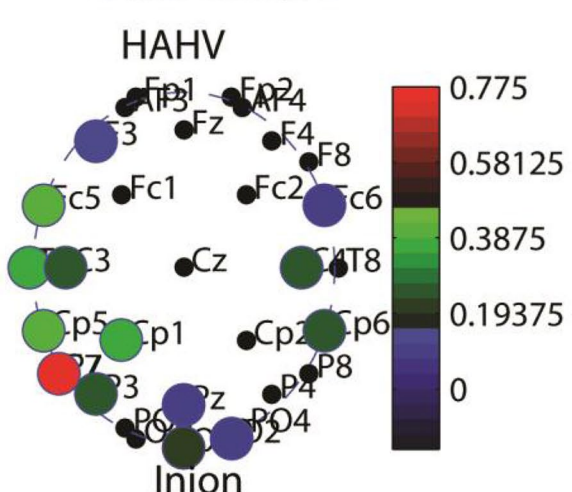
which obtained higher accuracies for separating low and high valence levels were selected. The color allocated to each node indicated the hubness of that node

the subject self-rating). These plots highlighted brain areas in which during negative emotions activated, while considering the classification results (see Fig. 2), since the maximum discrimination was obtained with positive emotions in the frequency band mentioned above each plot, it was considered that these highly activated brain areas were specific to negative emotions.

In Fig. 5, the average betweenness centrality of each node of MST graphs of all participants which were constructed based on EEG data of trials labeled with high valence level in DEAP dataset was displayed. The frequency band and connectivity metric were selected according to higher obtained accuracies for classification (see Fig. 3, lower panel). It should be noted that since in frequency band mentioned above each graph low and high arousal levels were separated with a high accuracy, it was assumed that the

highly activated centers in Fig. 5 (red circles) were specific to positive emotional states.

In Fig. 6, the average betweenness centrality (between 32 subjects and for EEG signals of emotions labeled as HAHV) was displayed. For constructing MST graph, frequency band and connectivity metric which obtained higher classification accuracy were used (see Fig. 3 upper panel). The selection of LALV (negative emotions) and HAHV (positive emotions) in Figs. 4, 5, and 6 were done according to the experimental evidences that existed in literature for emotional states and brain activities (see discussion section).

**Whole Frequency band/ PLI/10S****Whole Frequency band/MI/10s****Gamma/MI/5s****Beta/Corr/5s****Gamma/MI/2s****Beta/Corr/2s**

**Fig. 6** Pattern of average betweenness centrality for emotions labeled as HAHV. Averaging was performed between 32 subjects. The frequency band, connectivity metric and window size for constructing MST graph were specified above each panel

## Discussion

### Classification results

Figure 3 (upper panel) showed that maximum accuracy for arousal level discrimination was obtained for the window size of 10 s. Using the connectivity measure of PLI in the whole frequency range (4–45 Hz), the accuracy of 88.28% was achieved while the accuracy using MI connectivity metric in the alpha2 frequency band (10.5–12 Hz) was 80.46%. In contrast, for window sizes of 5 and 2 s, maximum accuracy was obtained using MI in the gamma band (81.25%) and Corr metric in the beta band (77.43%). Results in Fig. 3 (upper panel) indicated that the classification accuracy depended on the window size. Nevertheless, for discrimination of arousal levels (Fig. 3 upper panel), when window size changed from 2 to 5 s, the classification accuracy and the most significant frequency bands almost remained unchanged (except for the WPLI metric). On the other hand, discrimination between high and low valence levels changed considerably when the window size was changed from 2 to 5 s, however, the most significant frequency bands remained still unchanged (Fig. 3 lower panel). The higher discrimination accuracy for the valence level was achieved for a window size of 2 s, while connectivity was extracted using the Pcorr in the lower alpha band and for the window size of 5 s using WPLI in the gamma band.

Higher discrimination accuracy based on arousal level in the gamma frequency band (5 s and 2 s window size) might indicate that in excited compared with the neutral condition, information was encoded in higher frequency ranges like gamma [49, 50]. Figure 3 showed that the overall accuracy of emotion discrimination based on valence level was lower compared with arousal. The higher accuracy of emotion discrimination using arousal level was reported in other studies [26, 52]. Since the entropy content of EEG time series (data complexity) changed more considerably between low/high arousal levels compared with valence levels (see Table S1 in the supplementary material), distinguishing between different arousal levels could be obtained more accurately. This justified the higher accuracy of discrimination based on arousal level. Furthermore, several other studies reported that in the excited states the beta band of EEG signal was of significant importance [29, 69]. This was confirmed by the obtained results, where in Fig. 3 for 5 s and 2 s window size the discrimination accuracy for arousal level in beta and gamma bands was relatively higher than other frequency bands. The sensitivity of the entropy level of EEG time-series to emotional states made MI a suitable connectivity metric for computing connections between

different brain regions. Figure 3 showed that MI obtained more stable discrimination accuracy compared with other connectivity tools.

In comparison with other methods, Jie et al. obtained 80.43% and 71.16% for HAHV/HALV and HALV/LALV classification, respectively, which were lower than our proposed method. In their work, the Kolmogorov–Smirnov test was used for selecting some sample entropy coefficients calculated for the limited number of EEG channels [68]. Zhang et al. used sample entropy coefficients of intrinsic mode functions (IMFs) for two EEG channels (F3 and C4) which were filtered in the beta frequency band [29]. The classification accuracy for LAHV/HAHV, LAHV/LALV, HALV/LALV and HAHV/HALV was 93.92%, 93.40%, 95.63% and 96%, respectively. These accuracies were relatively higher than the proposed method in this paper.

According to Table 2, the classification accuracy for distinguishing different emotions from each other depended on the frequency content of EEG time series. This might indicate that the information of different emotions was encoded in different frequency bands of EEG time-series. If this is true, the multiclass classification in a distinct frequency range will result in a poor classification/discrimination accuracy.

The result of Table 3 showed that the proposed MST based method, which considered the interaction between several pairs of electrodes, obtained an accuracy of 88.28% and 81.25% for distinguishing emotions based on arousal and valence levels, respectively. The advantage of MST based method was that it could be used for both emotion recognition and study the information flow in brain circuits during emotion processing. The result in Table 3 showed that compared with the selection of some limited numbers of electrode pairs, when the interaction between different brain regions was considered, higher classification accuracy could be obtained. The involvement of different brain regions and their interactions during emotion processing [70] might support this better classification accuracy.

Furthermore, as Table S1 in supporting material indicated, the entropy which accounts for the information content of a time series was better measure than energy or phase information of EEG data for discriminating emotional states. This was supported by obtained results (Fig. 3) in which among connectivity measures, MI, a measure of information content, obtained relatively more stable classification accuracy in different window sizes.

### Evaluation of the classification outcomes and searching for important frequency bands

In the result section, the discrimination between emotional states using MST extracted features was considered. However, it is not clear if information regarding emotional states



is encoded at the specific-frequency band of EEG time-series. Here, according to the calculations performed in this study, we tried to search for a clear answer to such a question.

It was shown that during negative emotion processing the right brain hemisphere exhibited higher activity compared with the left side [20, 36]. This might indicate that during negative emotion processing significant hubs should be found in the right brain hemisphere. Negative emotions such as depression and sadness had low valence level and could be categorized in LALV area in arousal-valence space (see Fig. 1). According to the reported result in Fig. 3, the best classification result based on valence level was obtained in the alpha1 band (MI) for 10 s window size, gamma band (WPLI) for 5 s window size and alpha1 band (Pcorr) for 2 s window size. The hubness of MST graph nodes for the above-mentioned frequency bands and connectivity metrics was shown in Fig. 4. This figure showed that the presence of a highly connected node in the right hemisphere was observed when WPLI connectivity metric and gamma frequency band or Pcorr and alpha1 frequency band was used. The importance of C4 recording location was clear as the main hub for information flow during negative emotion processing. Before this high emotion discrimination results were obtained by Zhang et al. by considering only C4 and F3 electrodes [29]. The weight of the hub in the right side of the brain during low valence level when alpha1 frequency content of EEG time-series was used for MST generation was relatively higher than the gamma frequency band. The brain activity in the alpha band during negative emotion was reported by several studies [71, 72]. Besides this, the valence specific hypothesis suggested that the left hemisphere is a dominant player for processing positive affect while the negative effects are mainly processed by the right hemisphere [73], as it was reflected by Fig. 5 in case of alpha and gamma frequency bands. Altogether, it could be concluded that the alpha1 frequency band was the most informative band during negative emotion processing.

In the central area of the head, the strong correlation between positive emotions and brain activity in alpha (in the frontal region) and beta (in the right parietal region) band was observed [74, 75]. This correlation was satisfied by the current study when the alpha1 frequency band using partial correlation was used, while for other frequency bands it was not satisfied. The results based on DEAP dataset in Figs. 4 and 5 showed that the brain performed the main information processing task for emotions with both high and low valence levels in the alpha1 frequency band. Also, the classification results in Fig. 3 combined with reported results in Figs. 4 and 5 suggested that a 2 s window size might be an optimal choice for emotion classification based on valence level.

Furthermore, there were several studies that reported high activity in right parietal regions when the level of

arousal was high (i.e. HAHV and HALV quadrant of arousal-valence space [76, 77]). The emotions such as happiness, excited and anger could be categorized into high arousal regions of arousal-valence space. Also, there were several studies which reported the dominant role of the right hemisphere for processing positive emotions [64, 78], which could be categorized in the HAHV quadrant of arousal-valence space. Even though according to Fig. 3 (upper panel) the higher classification accuracy for arousal level was obtained for 10 s window size in the whole frequency range of EEG data, the presence of strong right parietal hub was only observed in the gamma frequency band (Fig. 6, Gamma/MI/2 s). This indicated that the main information of the emotions with high arousal level was encoded in the gamma frequency band of EEG data, while low arousal level emotion processing was performed in other frequency bands, due to the higher classification accuracy in the whole frequency band of data.

## Conclusion

In the present work, a graph theoretical approach was proposed for emotion recognition using EEG time-series. The MST graph was constructed from EEG data in brain frequency bands. Features of the MST graph were used for discrimination of emotions. The results showed that the classification accuracy of the proposed method was better than several existing state-of-the-art methods. Also, the classification accuracy was highly dependent on the frequency band of EEG data. This might be justified by the fact that different brain subsystems are engaged in distinct emotion processing tasks. These subsystems should be localized and work in a specific frequency range, therefore, their activities could alter the frequency content of EEG data. Our findings showed that the main frequency band regarding recognition of emotional stimuli with high arousal level was the gamma band (30–45 Hz), while alpha1 (8–10 Hz) was the most informative frequency band for preserving information regarding the valence level. Furthermore, the results of this study indicated that the optimal window size of EEG data for discrimination of valence level was 2 s and for recognition of arousal level it was 10 s. Nevertheless, at least a window size of 2 s of EEG data was required to simultaneously recognize arousal and valence levels. The advantage of MST graph for emotion classification over other existing methods which concentrate on the limited number of EEG electrodes was that it allowed studying dynamical states of the brain during emotion processing tasks. Moreover, it could help to understand the way that brain network complexity changed upon switching between emotional states.

## Compliance with ethical standards

**Conflict of interest** All authors declare that they have no conflict of interest.

**Ethical approval** All procedures performed in studies involving human participants were in accordance with the ethical standards of the institutional and/or national research committee and with the 1964 Helsinki declaration and its later amendments or comparable ethical standards.

**Informed consent** Informed consent was obtained from all individual participants included in the study.

## References

1. Harischandra J, Perera M (2012) Intelligent emotion recognition system using brain signals (EEG). In: 2012 IEEE EMBS conference on biomedical engineering and sciences (IECBES). IEEE, pp 454–459. <https://doi.org/10.1109/IECBES.2012.6498050>
2. Morin C (2011) Neuromarketing: the new science of consumer behavior. *Society* 48(2):131–135. <https://doi.org/10.1007/s12115-010-9408-1>
3. Feng C, Li W, Hu J, Yu K, Zhao D (2020) BCEFCM\_S: bias correction embedded fuzzy c-means with spatial constraint to segment multiple spectral images with intensity inhomogeneities and noises. *Signal Process* 168:107347. <https://doi.org/10.1016/j.sigpro.2019.107347>
4. Fieker M, Moritz S, Köther U, Jelinek L (2016) Emotion recognition in depression: an investigation of performance and response confidence in adult female patients with depression. *Psychiatry Res* 242:226–232. <https://doi.org/10.1016/j.psychres.2016.05.037>
5. Ricciardi L, Visco-Comandini F, Erro R, Morgante F, Bologna M, Fasano A, Ricciardi D, Edwards MJ, Kilner J (2017) Facial emotion recognition and expression in Parkinson's disease: an emotional mirror mechanism? *PLoS ONE* 12(1):e0169110. <https://doi.org/10.1371/journal.pone.0169110>
6. Fridenson-Hayo S, Berggren S, Lassalle A, Tal S, Pigat D, Bölte S, Baron-Cohen S, Golan O (2016) Basic and complex emotion recognition in children with autism: cross-cultural findings. *Mol Autism* 7(1):52. <https://doi.org/10.1186/s13229-016-0113-9>
7. Cowie R, Douglas-Cowie E, Tsapatsoulis N, Votsis G, Kollias S, Fellenz W, Taylor JG (2001) Emotion recognition in human-computer interaction. *IEEE Signal Proc Mag* 18(1):32–80. <https://doi.org/10.1109/79.911197>
8. Novak MJ, Warren JD, Henley SM, Draganski B, Frackowiak RS, Tabrizi SJ (2012) Altered brain mechanisms of emotion processing in pre-manifest Huntington's disease. *Brain* 135(4):1165–1179. <https://doi.org/10.1093/brain/aww024>
9. Yamada M, Murai T, Sato W, Namiki C, Miyamoto T, Ohigashi Y (2005) Emotion recognition from facial expressions in a temporal lobe epileptic patient with ictal fear. *Neuropsychologia* 43(3):434–441. <https://doi.org/10.1016/j.neuropsychologia.2004.06.019>
10. Dodich A, Cerami C, Canessa N, Crespi C, Marcone A, Arpone M, Realmuto S, Cappa SF (2014) Emotion recognition from facial expressions: a normative study of the Ekman 60-faces test in the Italian population. *Neurol Sci* 35(7):1015–1021. <https://doi.org/10.1007/s10072-014-1631-x>
11. McCubbin JA, Merritt MM, Sollers JJ 3rd, Evans MK, Zonderman AB, Lane RD, Thayer JF (2011) Cardiovascular-emotional dampening: the relationship between blood pressure and recognition of emotion. *Psychosom Med* 73(9):743–750. <https://doi.org/10.1097/PSY.0b013e318235ed55>
12. Balconi M, Vanutelli ME (2016) Hemodynamic (fNIRS) and EEG (N200) correlates of emotional inter-species interactions modulated by visual and auditory stimulation. *Sci Rep* 6:23083. <https://doi.org/10.1038/srep23083>
13. Selvaraj J, Murugappan M, Wan K, Yaacob S (2013) Classification of emotional states from electrocardiogram signals: a non-linear approach based on hurst. *Biomed Eng Online* 12:44–44. <https://doi.org/10.1186/1475-925X-12-44>
14. Nwe TL, Foo SW, De Silva LC (2003) Speech emotion recognition using hidden Markov models. *Speech Commun* 41(4):603–623. [https://doi.org/10.1016/S0167-6393\(03\)00099-2](https://doi.org/10.1016/S0167-6393(03)00099-2)
15. Nakasone A, Prendinger H, Ishizuka M (2013) Emotion recognition from electromyography and skin conductance. In: *Proceedings of the 5th international workshop on biosignal interpretation*. Citeseer, pp 219–222
16. Yin Z, Zhao M, Wang Y, Yang J, Zhang J (2017) Recognition of emotions using multimodal physiological signals and an ensemble deep learning model. *Comput Methods Prog Biol* 140:93–110. <https://doi.org/10.1016/j.cmpb.2016.12.005>
17. Golnar-Nik P, Farashi S, Safari M-S (2019) The application of EEG power for the prediction and interpretation of consumer decision-making: a neuromarketing study. *Physiol Behav* 207:90–98. <https://doi.org/10.1016/j.physbeh.2019.04.025>
18. Dennis TA, Hajcak G (2009) The late positive potential: a neuro-physiological marker for emotion regulation in children. *J Child Psychol Psychiatry* 50(11):1373–1383. <https://doi.org/10.1111/j.1469-7610.2009.02168.x>
19. Konstantinidis EI, Frantzidis CA, Pappas C, Bamidis PD (2012) Real time emotion aware applications: a case study employing emotion evocative pictures and neuro-physiological sensing enhanced by graphic processor units. *Comput Methods Prog Biol* 107(1):16–27. <https://doi.org/10.1016/j.cmpb.2012.03.008>
20. Demaree HA, Everhart DE, Youngstrom EA, Harrison DW (2005) Brain lateralization of emotional processing: historical roots and a future incorporating “dominance”. *Behav Cognit Neurosci Rev* 4(1):3–20. <https://doi.org/10.1177/1534582305276837>
21. Khosrowabadi R, Bin Abdul Rahman AW (2010) Classification of EEG correlates on emotion using features from Gaussian mixtures of EEG spectrogram. In: *2010 international conference on information and communication technology for the Muslim world (ICT4M)*. IEEE, pp E102–E107. <https://doi.org/10.1109/ICT4M.2010.5971942>
22. Othman M, Wahab A, Khosrowabadi R (2009) MFCC for robust emotion detection using EEG. In: *2009 IEEE 9th Malaysia international conference on communications (MICC)*, 2009. IEEE, pp 98–101. <https://doi.org/10.1109/MICC.2009.5431473>
23. Kumar N, Khaund K, Hazarika SM (2016) Bispectral analysis of EEG for emotion recognition. *Procedia Comput Sci* 84:31–35. <https://doi.org/10.1016/j.procs.2016.04.062>
24. Lee G, Kwon M, Kavuri Sri S, Lee M (2014) Emotion recognition based on 3D fuzzy visual and EEG features in movie clips. *Neurocomputing* 144:560–568. <https://doi.org/10.1016/j.neucom.2014.04.008>
25. Khosrowabadi R, Quek C, Ang KK, Wahab A (2014) ERNN: a biologically inspired feedforward neural network to discriminate emotion from EEG signal. *IEEE Trans Neural Netw Learn Syst* 25(3):609–620. <https://doi.org/10.1109/TNNLS.2013.2280271>
26. Mohammadi Z, Frounchi J, Amiri M (2016) Wavelet-based emotion recognition system using EEG signal. *Neural Comput Appl*. <https://doi.org/10.1007/s00521-015-2149-8>
27. Farashi S (2018) Spike detection using a multiresolution entropy based method. *Biomed Eng Biomed Tech* 63(4):361–376. <https://doi.org/10.1515/bmt-2016-0182>

28. Farashi S, Abolhassani MD, Salimpour Y, Alirezaie J (2010) Combination of PCA and undecimated wavelet transform for neural data processing. In: 2010 annual international conference of the IEEE engineering in medicine and biology. IEEE, pp 6666–6669. <https://doi.org/10.1109/IEMBS.2010.5627158>
29. Zhang Y, Ji X, Zhang S (2016) An approach to EEG-based emotion recognition using combined feature extraction method. *Neurosci Lett* 633:152–157. <https://doi.org/10.1016/j.neulet.2016.09.037>
30. Liu Y, Sourina O, Nguyen MK (2011) Real-time EEG-based emotion recognition and its applications. In: Transactions on computational science XII. Springer, pp 256–277. [https://doi.org/10.1007/978-3-642-22336-5\\_13](https://doi.org/10.1007/978-3-642-22336-5_13)
31. Petrantonakis PC, Hadjileontiadis LJ (2010) Emotion recognition from EEG using higher order crossings. *IEEE Trans Inf Theory* 14(2):186–197. <https://doi.org/10.1109/TITB.2009.2034649>
32. Eryilmaz H, Van De Ville D, Schwartz S, Vuilleumier P (2011) Impact of transient emotions on functional connectivity during subsequent resting state: a wavelet correlation approach. *Neuroimage* 54(3):2481–2491. <https://doi.org/10.1016/j.neuroimage.2010.10.021>
33. Khosrowabadi R, Quek HC, Wahab A, Ang KK (2010) EEG-based emotion recognition using self-organizing map for boundary detection. In: 2010 20th international conference on pattern recognition (ICPR). IEEE, pp 4242–4245. <https://doi.org/10.1109/ICPR.2010.1031>
34. Atkinson J, Campos D (2016) Improving BCI-based emotion recognition by combining EEG feature selection and kernel classifiers. *Expert Syst Appl* 47:35–41. <https://doi.org/10.1016/j.eswa.2015.10.049>
35. Costa T, Rognoni E, Galati D (2006) EEG phase synchronization during emotional response to positive and negative film stimuli. *Neurosci Lett* 406(3):159–164. <https://doi.org/10.1016/j.neulet.2006.06.039>
36. Xing M, Tadayonnejad R, MacNamara A, Ajilore O, DiGangi J, Phan KL, Leow A, Klumpp H (2017) Resting-state theta band connectivity and graph analysis in generalized social anxiety disorder. *NeuroImage Clin* 13:24–32. <https://doi.org/10.1016/j.nicl.2016.11.009>
37. Feng C, Zhao D, Huang M (2016) Segmentation of longitudinal brain MR images using bias correction embedded fuzzy c-means with non-locally spatio-temporal regularization. *J Vis Commun Image Represent* 38:517–529. <https://doi.org/10.1016/j.jvcir.2016.03.027>
38. Feng C, Zhao D, Huang M (2016) Image segmentation using CUDA accelerated non-local means denoising and bias correction embedded fuzzy c-means (BCEFCM). *Signal Process* 122:164–189. <https://doi.org/10.1016/j.sigpro.2015.12.007>
39. Vourkas M, Karakonstantaki E, Simos PG, Tsirka V, Antonakakis M, Vamvoukas M, Stam C, Dimitriadis S, Micheloyannis S (2014) Simple and difficult mathematics in children: a minimum spanning tree EEG network analysis. *Neurosci Lett* 576:28–33. <https://doi.org/10.1016/j.neulet.2014.05.048>
40. Fraga González G, Van der Molen MJW, Žarić G, Bonte M, Tijms J, Blomert L, Stam CJ, Van der Molen MW (2016) Graph analysis of EEG resting state functional networks in dyslexic readers. *Clin Neurophysiol* 127(9):3165–3175. <https://doi.org/10.1016/j.clinph.2016.06.023>
41. Fraschini M, Demuru M, Hillebrand A, Cuccu L, Porcu S, Di Stefano F, Puligheddu M, Floris G, Borghero G, Marrosu F (2016) EEG functional network topology is associated with disability in patients with amyotrophic lateral sclerosis. *Sci Rep* 6:38653. <https://doi.org/10.1038/srep38653>
42. Alessandra C, Matteo D, Luca D, Gian Luca M, Matteo F (2016) Minimum spanning tree and k -core decomposition as measure of subject-specific EEG traits. *Biomed Phys Eng Express* 2(1):017001
43. Demuru M, Fara F, Fraschini M (2013) Brain network analysis of EEG functional connectivity during imagery hand movements. *J Integr Neurosci* 12(04):441–447. <https://doi.org/10.1142/S021963521350026X>
44. van Dellen E, de Waal H, Flier WM, Lemstra AW, Slooter AJ, Smits LL, van Straaten EC, Stam CJ, Scheltens P (2015) Loss of EEG network efficiency is related to cognitive impairment in dementia with Lewy bodies. *Movement Disord* 30(13):1785–1793. <https://doi.org/10.1002/mds.26309>
45. van Dellen E, Douw L, Hillebrand A, de Witt Hamer PC, Baayen JC, Heimans JJ, Reijneveld JC, Stam CJ (2014) Epilepsy surgery outcome and functional network alterations in longitudinal MEG: a minimum spanning tree analysis. *Neuroimage* 86:354–363. <https://doi.org/10.1016/j.neuroimage.2013.10.010>
46. Klimesch W (2012) Alpha-band oscillations, attention, and controlled access to stored information. *Trends Cogn Sci* 16(12):606–617. <https://doi.org/10.1016/j.tics.2012.10.007>
47. Sauseng P, Griesmayr B, Freunberger R, Klimesch W (2010) Control mechanisms in working memory: a possible function of EEG theta oscillations. *Neurosci Biobehav Rev* 34(7):1015–1022. <https://doi.org/10.1016/j.neubiorev.2009.12.006>
48. Zhang X, Kendrick KM, Zhou H, Zhan Y, Feng J (2012) A computational study on altered theta-gamma coupling during learning and phase coding. *PLoS ONE* 7(6):e36472. <https://doi.org/10.1371/journal.pone.0036472>
49. Muller MM, Keil A, Gruber T, Elbert T (1999) Processing of affective pictures modulates right-hemispheric gamma band EEG activity. *Clin Neurophysiol* 110(11):1913–1920. [https://doi.org/10.1016/S1388-2457\(99\)00151-0](https://doi.org/10.1016/S1388-2457(99)00151-0)
50. Luo Q, Mitchell D, Cheng X, Mondillo K, McCaffrey D, Holroyd T, Carver F, Coppola R, Blair J (2009) Visual awareness, emotion, and gamma band synchronization. *Cereb Cortex* 19(8):1896–1904. <https://doi.org/10.1093/cercor/bhn216>
51. Russell JA, Weiss A, Mendelsohn GA (1989) Affect grid: a single-item scale of pleasure and arousal. *J Pers Soc Psychol* 57(3):493. <https://doi.org/10.1037/0022-3514.57.3.493>
52. Koelstra S, Muhl C, Soleymani M, Lee J-S, Yazdani A, Ebrahimi T, Pun T, Nijholt A, Patras I (2012) Deap: a database for emotion analysis; using physiological signals. *IEEE Trans Affect Comput* 3(1):18–31. <https://doi.org/10.1109/T-AFCC.2011.15>
53. Klimesch W (1999) EEG alpha and theta oscillations reflect cognitive and memory performance: a review and analysis. *Brain Res Brain Res Rev* 29(2–3):169–195. [https://doi.org/10.1016/S0165-0173\(98\)00056-3](https://doi.org/10.1016/S0165-0173(98)00056-3)
54. Stam CJ (2000) Brain dynamics in theta and alpha frequency bands and working memory performance in humans. *Neurosci Lett* 286(2):115–118. [https://doi.org/10.1016/S0304-3940\(00\)01109-5](https://doi.org/10.1016/S0304-3940(00)01109-5)
55. Davidson RJ, Ekman P, Saron CD, Senulis JA, Friesen WV (1990) Approach-withdrawal and cerebral asymmetry: emotional expression and brain physiology. *Int J Pers Soc Psychol* 58(2):330–341. <https://doi.org/10.1037/0022-3514.58.2.330>
56. Candra H, Yuwono M, Chai R, Handojoseno A, Elamvazuthi I, Nguyen HT, Su S (2015) Investigation of window size in classification of EEG-emotion signal with wavelet entropy and support vector machine. In: Proceeding of the conference of the IEEE engineering in medicine and biology society, 2015. IEEE, pp 7250–7253. <https://doi.org/10.1109/EMBC.2015.7320065>
57. Bowyer SM (2016) Coherence a measure of the brain networks: past and present. *Neuropsychiatr Electrophysiol* 2(1):1. <https://doi.org/10.1186/s40810-015-0015-7>
58. Na SH, Jin S-H, Kim SY, Ham B-J (2002) EEG in schizophrenic patients: mutual information analysis. *Clin*

- Neurophysiol 113(12):1954–1960. [https://doi.org/10.1016/S1388-2457\(02\)00197-9](https://doi.org/10.1016/S1388-2457(02)00197-9)
59. Smith SM, Miller KL, Salimi-Khorshidi G, Webster M, Beckmann CF, Nichols TE, Ramsey JD, Woolrich MW (2011) Network modelling methods for FMRI. *Neuroimage* 54(2):875–891. <https://doi.org/10.1016/j.neuroimage.2010.08.063>
  60. Nolte G, Bai O, Wheaton L, Mari Z, Vorbach S, Hallett M (2004) Identifying true brain interaction from EEG data using the imaginary part of coherency. *Clin Neurophysiol* 115(10):2292–2307. <https://doi.org/10.1016/j.clinph.2004.04.029>
  61. Stam CJ, Nolte G, Daffertshofer A (2007) Phase lag index: assessment of functional connectivity from multichannel EEG and MEG with diminished bias from common sources. *Hum Brain Mapp* 28(11):1178–1193. <https://doi.org/10.1002/hbm.20346>
  62. Vinck M, Oostenveld R, Van Wingerden M, Battaglia F, Pennartz CM (2011) An improved index of phase-synchronization for electrophysiological data in the presence of volume-conduction, noise and sample-size bias. *Neuroimage* 55(4):1548–1565. <https://doi.org/10.1016/j.neuroimage.2011.01.055>
  63. Nolte G, Ziehe A, Krämer N, Popescu F, Müller K-R (2010) Comparison of granger causality and phase slope index. In: *Causality: objectives and assessment*, pp 267–276
  64. Pettie S, Ramachandran V (2002) An optimal minimum spanning tree algorithm. *J ACM* 49(1):16–34. [https://doi.org/10.1007/3-540-45022-X\\_6](https://doi.org/10.1007/3-540-45022-X_6)
  65. Newman ME (2005) A measure of betweenness centrality based on random walks. *Social Netw* 27(1):39–54. <https://doi.org/10.1016/j.socnet.2004.11.009>
  66. Boersma M, Smit DJ, Boomsma DI, De Geus EJ, Delemarre-van de Waal HA, Stam CJ (2013) Growing trees in child brains: graph theoretical analysis of electroencephalography-derived minimum spanning tree in 5- and 7-year-old children reflects brain maturation. *Brain Connect* 3(1):50–60. <https://doi.org/10.1089/brain.2012.0106>
  67. Faul F, Erdfelder E, Lang AG, Buchner A (2007) G\*Power 3: a flexible statistical power analysis program for the social, behavioral, and biomedical sciences. *Behav Res Methods* 39(2):175–191. <https://doi.org/10.3758/bf03193146>
  68. Jie X, Cao R, Li L (2014) Emotion recognition based on the sample entropy of EEG. *Bio-Med Mater Eng* 24(1):1185–1192. <https://doi.org/10.3233/bme-130919>
  69. Güntekin B, Başar E (2010) Event-related beta oscillations are affected by emotional eliciting stimuli. *Neurosci Lett* 483(3):173–178. <https://doi.org/10.1016/j.neulet.2010.08.002>
  70. Esslen M, Pascual-Marqui R, Hell D, Kochi K, Lehmann D (2004) Brain areas and time course of emotional processing. *Neuroimage* 21(4):1189–1203. <https://doi.org/10.1016/j.neuroimage.2003.10.001>
  71. Lee Y-Y, Hsieh S (2014) Classifying different emotional states by means of EEG-based functional connectivity patterns. *PLoS ONE* 9(4):e95415. <https://doi.org/10.1371/journal.pone.0095415>
  72. Wang N, Wei L, Li Y (2012) Analysis of characteristics of alpha electroencephalogram during the interaction between emotion and cognition based on Granger causality. *Sheng Wu Yi Xue Gong Cheng Xue Za Zhi* 29(6):1021–1026
  73. Killgore WDS, Yurgelun-Todd DA (2007) The right-hemisphere and valence hypotheses: could they both be right (and sometimes left)? *Soc Cogn Affect Neurosci* 2(3):240–250. <https://doi.org/10.1093/scan/nsm020>
  74. Bos DO (2006) EEG-based emotion recognition. In: *The influence of visual and auditory stimuli*, pp 1–17
  75. Hu X, Yu J, Song M, Yu C, Wang F, Sun P, Wang D, Zhang D (2017) EEG correlates of ten positive emotions. *Front Hum Neurosci* 11:26. <https://doi.org/10.3389/fnhum.2017.00026>
  76. Brooks JR, Garcia JO, Kerick SE, Vettel JM (2016) Differential functionality of right and left parietal activity in controlling a motor vehicle. *Front Syst Neurosci* 10:106. <https://doi.org/10.3389/fnsys.2016.00106>
  77. Engels AS, Heller W, Mohanty A, Herrington JD, Banich MT, Webb AG, Miller GA (2007) Specificity of regional brain activity in anxiety types during emotion processing. *Psychophysiology* 44(3):352–363. <https://doi.org/10.1111/j.1469-8986.2007.00518.x>
  78. Kuchinke L, Lux V (2012) Caffeine improves left hemisphere processing of positive words. *PLoS ONE* 7(11):e48487. <https://doi.org/10.1371/journal.pone.0048487>

**Publisher's Note** Springer Nature remains neutral with regard to jurisdictional claims in published maps and institutional affiliations.